

# Moving contact line with balanced stress singularities

X. Y. Hu and N. A. Adams

*Lehrstuhl für Aerodynamik, Technische Universität München  
85748 Garching, Germany*

---

## Abstract

A difficulty in the classical hydrodynamic analysis of moving contact-line problems, associated with the no-slip wall boundary condition resulting in an unbalanced divergence of the viscous stresses, is reexamined with a smoothed, finite-width interface model. The analysis in the sharp-interface limit shows that the singularity of the viscous stress can be balanced by another singularity of the unbalanced surface stress. The dynamic contact angle is determined by surface tension, viscosity, contact-line velocity and a single non-dimensional parameter reflecting the length-scale ratio between interface width and the thickness of the first molecule layer at the wall surface. The widely used Navier boundary condition and Cox's hypothesis are also derived following the same procedure by permitting finite-wall slip.

*Key words:* moving contact line, boundary condition, dynamic contact angle

---

## 1 Introduction

Immiscible two-phase flows with moving contact lines occur in a variety of applications, such as coating and biological processes. The moving contact line problem, however, has for many years remained a partially open issue. One of the problems is the validity of the no-slip wall boundary condition, which arises with classical hydrodynamics, where for a no-slip wall an unbalanced divergence of the viscous stress occurs, which leads to a violation of the contact-angle condition at a moving contact line [8][5]. There have been many attempts to resolve the problem by modifying the boundary condition, including the slip model [6][18], the interface relaxation model [15], the diffusive interface model [10] [3], and the combined molecular-dynamics and diffusive-interface model [14]. However, studies by molecular dynamics show that even though considerable contact-line velocities can be obtained [11] [16], the maxi-

mum shear rate is still many orders less than that which can violate the no-slip wall boundary condition considerably [17].

## 2 Smoothed, finite-width interface model for moving contact line

In this Letter, we reexamine the hydrodynamics of a fluid/fluid/solid system with a steady moving contact line. Instead of considering sharp interfaces directly, our analysis starts from smoothed, finite-width interfaces. Given the continuous interfacial free energy density with the form [9]  $f = \frac{1}{2}\sigma|\nabla C|^2 + \Psi(C)$ , where  $C$  is a color function,  $\sigma$  is a coefficient and  $\Psi(C)$  is the bulk energy density, at the state which minimizes  $\mathcal{F} = \int f dV$  the interface reaches its equilibrium profile. In this case the surface stress  $\Pi_{ij}$  in a two dimensional Cartesian coordinate system is given by

$$\Pi_{ij} = \sigma \left( \delta_{ij} \frac{\partial C}{\partial x_k} \frac{\partial C}{\partial x_k} - \frac{\partial C}{\partial x_i} \frac{\partial C}{\partial x_j} \right), \quad i, j, k = 1, 2 \quad (1)$$

where  $\delta_{ij}$  is the Kronecker delta. One important property of the surface stress is that one of the principle axes  $x'_1$  is aligned with the gradient of the color function, the other principle axis  $x'_2$  is aligned with the interface tangential direction, along which the only non-zero component of the surface stress is the positive normal stress (tension),  $\Pi_{2'2'} = \sigma|\nabla C|^2$ . The relation between the surface tension  $\gamma$  and  $\sigma$  for an infinite plane interface is given by

$$\gamma = \sigma \int_{-\infty}^{+\infty} \Pi_{2'2'} dx'_1. \quad (2)$$

We consider a steady moving contact line with dynamic contact angle  $\alpha$ , and velocity  $U_s$ , as shown in Fig. 1. Around the contact line there are three phases: fluid 1, fluid 2 and the static wall. We define the color function as

$$C^{kl} = \begin{cases} 1 & \text{in phase } l \\ 0 & \text{else} \end{cases}, \quad k, l = 1, 2, w. \quad (3)$$

Note that the color function is discontinuous across the interfaces. In order to obtain a finite, continuous surface stress, we introduce a two-dimensional smoothing-kernel function [13] [12]

$$W(\mathbf{x}, \xi) = \frac{1}{\xi^2 \pi} e^{-\mathbf{x}^2/\xi^2} \quad (4)$$

in which  $\xi$  is smoothing length and  $\xi \ll L$ ,  $L$  is the characteristic length scale of the system.  $W(\mathbf{x}, \xi)$  is radially symmetric and has the properties  $\int W(\mathbf{x} - \mathbf{x}', \xi) d\mathbf{x} = 1$  and  $\lim_{\xi \rightarrow 0} W(\mathbf{x} - \mathbf{x}', \xi) = \delta(\mathbf{x} - \mathbf{x}')$ . After convolution

with the kernel function, the smoothed gradient of the color function pointing towards phase  $l$  at a point  $\mathbf{x}'$  in phase  $k$  is

$$\nabla C^{kl}(\mathbf{x}') = \int C^{kl}(\mathbf{x}) \nabla W(\mathbf{x} - \mathbf{x}', \xi) d\mathbf{x}, l \neq k. \quad (5)$$

Assuming that the smoothed profile defined by  $\nabla C^{kl}(\mathbf{x}')$  is the interface profile corresponding to an equilibrium form of the bulk energy density, the total surface stress at a point in phase  $k$  is can be calculated from Eq. (1), by  $\Pi_{ij} = \sum_{l \neq k} \Pi_{ij}(\nabla C^{kl})$ . It is easy to verify by Eq. (2) that, for a infinite plane interface between phase  $k$  and phase  $l$ , the surface tension is

$$\gamma_{kl} = \frac{\sigma_{kl}}{\sqrt{2\pi\xi}}. \quad (6)$$

Figure 1 indicates the regions of non-vanishing  $\nabla C^{kl}$  for different phase pairings. Note that there are overlap regions near the contact line.

In order to study the contact-line dynamics, as shown in Fig. 1, we define a small square control volume with side length  $2\varepsilon$ ,  $\varepsilon \ll \xi$ , with one side on the wall surface so that the interface between the fluid 1 and fluid 2 goes through the control volume. Assuming incompressibility and straight interfaces with  $\alpha$  not far from  $\frac{\pi}{2}$ , we obtain

$$2\varepsilon \Pi_{11}^l + \int \Pi_{21}^w dx_1 + 2\varepsilon \tau_{11}^l + \int \tau_{21}^w dx_1 = 2\varepsilon \Pi_{11}^r + \int \Pi_{21}^f dx_1 + 2\varepsilon \tau_{11}^r + \int \tau_{21}^f dx_1, \quad (7)$$

by considering the force balance on the control volume in tangential (wall parallel) direction, where the superscripts  $l$ ,  $w$ ,  $r$  and  $f$  represent the left, wall, right and upper faces of the control volume.  $\Pi_{11}$  and  $\Pi_{21}$  are the tangential components of surface stress.  $\tau_{11}$  and  $\tau_{21}$  are the tangential components of viscous stress. As  $\varepsilon$  is small and  $\varepsilon \ll \xi$ , the gradients of the color functions at a point on the face of control volumes can be approximated with the representative values on the contact line. If the contact line is defined to be at the origin of a two-dimensional polar coordinate system, the gradient is given by

$$\nabla C^{kl}(\mathbf{x}' \rightarrow 0) = \int_{\Omega(\theta, \theta')} \nabla W(\mathbf{x}, \xi) d\mathbf{x}, l \neq k \quad (8)$$

where  $\Omega(\theta, \theta')$  represents the sector between polar angles  $\theta$  and  $\theta'$  in two-dimensional polar coordinates, and  $\theta, \theta' = 0, \alpha, \pi$  depending on the choice of phase pairs. It can be readily obtained that  $\int_{\Omega(\theta, \theta')} \nabla W(\mathbf{x}, \xi) d\mathbf{x} = (\sin \theta - \sin \theta', \cos \theta' - \cos \theta) \frac{1}{2\sqrt{\pi\xi}}$ . With Eq. (1), the tangential surface-stress components in Eq. (7) are  $\Pi_{11}^{12} = \frac{\sigma_{12}}{4\pi\xi^2}(1 - \cos \alpha)^2$ ,  $\Pi_{21}^{12} = \frac{\sigma_{12}}{4\pi\xi^2} \sin \alpha(\cos \alpha - 1)$ ,  $\Pi_{11}^{21} = \frac{\sigma_{12}}{4\pi\xi^2}(1 + \cos \alpha)^2$ ,  $\Pi_{21}^{21} = \frac{\sigma_{12}}{4\pi\xi^2} \sin \alpha(1 + \cos \alpha)$ ,  $\Pi_{11}^{1w} = \frac{\sigma_{1w}}{\pi\xi^2}$ ,  $\Pi_{21}^{1w} = 0$ ,  $\Pi_{11}^{2w} = \frac{\sigma_{2w}}{\pi\xi^2}$  and  $\Pi_{21}^{2w} = 0$ , where  $\sigma_{1w}$ ,  $\sigma_{2w}$  and  $\sigma_{12}$  are the coefficients between fluid 1 and wall, fluid 2 and wall, and fluid 1 and fluid 2. Hence, using Eq. (6),

Eq. (7) becomes

$$\gamma_{1w} + \sqrt{\frac{\pi}{2}} \xi \mu \left[ \left( \frac{\partial u_1}{\partial x_2} \right)^w - \left( \frac{\partial u_1}{\partial x_2} \right)^f + \left( \frac{\partial u_1}{\partial x_1} \right)^l - \left( \frac{\partial u_1}{\partial x_1} \right)^r \right] = \gamma_{2w} + \frac{1}{2} \gamma_{12} \cos \alpha \quad (9)$$

where  $\gamma_{1w}$ ,  $\gamma_{2w}$  and  $\gamma_{12}$  are the surface tensions between fluid 1 and wall, fluid 2 and wall, and fluid 1 and fluid 2, respectively. Note that, the shear rates on the faces of the control volume are approximated with the values on face-centers, and that the viscosities of fluid 1 and fluid 2 are assumed to have the same value  $\mu$ . When the fluids are in static equilibrium the second term on the left-hand-side disappears, Eq. (9) becomes

$$\gamma_{1w} = \gamma_{2w} + \frac{1}{2} \gamma_{12} \cos \alpha' \quad (10)$$

where  $\alpha'$  is the static contact angle. Eq. (10) implies that the static contact angle is different from that obtained by Young's relation, except  $\alpha' = \frac{\pi}{2}$ . This is not unexpected because the current relation gives the force balance within the interface. Note that for  $\alpha \neq \alpha'$ , an unbalanced surface stress along the tangential direction arises in Eq. (7), and is balanced by the differences between the shear stresses. To study the details of the balance between surface forces and viscous forces, it is convenient to define a layer, as shown in Fig. 1, which has a small thickness of  $\varepsilon$  and a velocity  $U_\varepsilon$  in the center of the control volume. As  $U_\varepsilon \rightarrow U_s$  for  $\varepsilon \rightarrow 0$ , one can study the force balance exactly at the contact line. For any location other than the contact line there is no unbalanced surface stress as in Eq. (7) and hence viscous forces are continuous. Therefore, it is straightforward to assume that the fluid velocity on the left and right faces of the control volume match continuously with the wall velocity, and the shear rate on the upper face of the control volume match continuously with that of the bulk flow. Here, three types of wall boundary conditions with different wall-slips, i.e. no-slip, finite-slip and free-slip, are to be considered.

### 3 Discussion

If a no-slip wall boundary condition is applied, the viscous stress is calculated from viscosity and shear rate. As  $\varepsilon$  is small, a linear approximation of the shear rates is sufficient, then Eq. (9) can be rewritten as

$$\Gamma \mu U_\varepsilon - \sqrt{2\pi} \xi \mu \left( \frac{\partial u_1}{\partial x_2} \right)^f = \sigma_{12} (\cos \alpha - \cos \alpha'). \quad (11)$$

where  $\Gamma = \sqrt{2\pi} \frac{\xi}{\varepsilon} \gg 1$  is a non-dimensional parameter. Note that the normal viscous stresses here cancel out because of opposite directions and same mag-

nitudes. For the distinguished limit of a sharp interface  $\Gamma \gg 1$  as  $\xi, \varepsilon \rightarrow 0$ , one has

$$\Gamma \text{Ca} = \cos \alpha - \cos \alpha' \quad (12)$$

where the capillary number is defined by  $\text{Ca} = \mu U_s / \gamma_{12}$ , since  $\left(\frac{\partial u_1}{\partial x_2}\right)^f \sim \frac{U}{L}$  is finite and  $U_\varepsilon \rightarrow U_s$ . Now that the same form as Eq. (12) with  $\Gamma = \sqrt{\frac{9\pi}{2}} \frac{\xi}{\varepsilon}$  can be derived if the viscosity of fluid 2 is neglected. Here, the problem discussed in Refs. [8] and [5] can be solved: for infinite viscous stress in Eq. (7) in the limit  $\varepsilon \rightarrow 0$ , Eq. (12) implies that there still is a contact-angle condition at the contact line for a non-vanishing contact-line velocity  $U_s$ . The reason is that, for  $\xi \rightarrow 0$  the unbalanced surface stress in Eq. (7) becomes infinite as well, and Eq. (12) gives the condition for which the two infinite stresses are in equilibrium. Note that the problem of a singular viscous force remains only if  $\varepsilon \rightarrow 0$  and  $\xi$  does not vanish. This limit results in  $U_s \rightarrow 0$ , i.e. the contact line does not move.

A straightforward interpretation of Eq. (12) with respect to the microscopic length scales indicates that  $\xi$  corresponds to the physical width of the interface and  $\varepsilon$  to the thickness of the first molecules layer at the wall surface, and  $\Gamma$  is just the ratio between the two length scales. Since the thickness of the first molecule layer is quite close to the molecule size and the interface width is at least several times the molecule size, our result  $\Gamma \gg 1$  is physically meaningful. Eq. (12) is derived from a classical hydrodynamic analysis in which the only considered dissipation mechanism is the viscous force. It is quite surprising that Eq. (12) has the same form as a linearized formulation of the molecular-kinetic model [1] which was proposed to discard dissipation due to viscous flow:  $\Gamma' \text{Ca} = (\cos \alpha - \cos \alpha')$ , where  $\Gamma' = \eta / \mu$ ,  $\eta$  is the coefficient of wetting-line friction. Note that  $\eta$  has the units of the viscosity  $\mu$ , and is always much larger than  $\mu$  [2], which is in agreement with our result  $\Gamma \gg 1$ . It is also interesting that Eq. (12) has the same form as the small-velocity-approximation relation of Shihkmuraev's interface relaxation model [15]. However, Shihkmuraev obtained a zero contact-line velocity for negligible interface relaxation, as opposite to finite contact-line velocity obtained in our current analysis.

If a finite-slip wall boundary condition is applied, the viscous stress on the wall for  $\varepsilon \rightarrow 0$  is given as  $\beta U_s$ , where  $\beta$  is the slip-coefficient. In this case Eq. (9) becomes

$$\beta U_s - \mu \left(\frac{\partial u_1}{\partial x_2}\right)^f = \sqrt{2\pi} \frac{\sigma_{12}}{\xi} (\cos \alpha - \cos \alpha'). \quad (13)$$

Eq. (13) is in agreement with the slip-wall boundary condition of Qian, Wang & Sheng [14], which states that the wall slip is proportional to the sum of the viscous stress and the uncompensated Young stress. An important result different from that of the sharp interface model is that for a given contact-line velocity the dynamic contact angle is strongly affected by the shear rate of

the bulk flow. Note that Eq. (13) is valid only for finite-thickness interfaces and implies a surface-force singularity if the interface thickness tends to zero. To eliminate the singularity the dynamic and static contact angles should be equal  $\alpha = \alpha'$ , which explains the underlying reason of Cox's hypothesis [4] for a macroscopic analysis stating that wall-slip is permitted and the contact angle is independent of contact-line velocity. A result of the surface-force balance with  $\alpha = \alpha'$  from Eq. (13) is the widely used Navier boundary condition  $U_s = \lambda \left( \frac{\partial u_1}{\partial x_2} \right)^f$ , where  $\lambda = \mu/\beta$  is the slip length.

Our analysis does not allow for a free-slip boundary condition [7] because free slip would result in the first term on the left-hand-side of Eq. (13) to vanish, which may lead to an un-physical decrease of the contact angle for an advancing contact line. For the sharp-interface limit with free slip there is no force balance, no matter whether the dynamic and static contact angles are the same or not.

## 4 Conclusion

To summarize, we have studied the force balance at a moving contact line with different boundary conditions. It is found that, for the sharp-interface limit, both the finite-slip and the no-slip wall boundary conditions are possible. With the finite-slip wall assumption, the analysis explains that the previously used Cox's hypothesis and the Navier boundary condition are essential for a force balance. However, the analysis also suggests that the no-slip wall boundary conditions is still valid along with a contact-angle condition, which agrees with several previous studies on dynamic contact angles. More importantly, since there is no conflict with the results of molecular dynamics simulations, the no-slip wall boundary condition can serve for obtaining more reliable numerical predictions of moving contact line problems.

## References

- [1] T. D. Blake. Dynamic contact angles and wetting kinetics. In J. C. Berg, editor, *Wettability*, New York, 1993. Marcel Dekker.
- [2] T. D. Blake. The physics of moving wetting lines. *J. Colloid Interface Sci.*, 299:1–13, 2006.
- [3] H. Y. Chen, D. Jasnow, and J. Vinals. Interface and contact line motion in a two phase fluid under shear flow. *Phys. Rev. Lett.*, 85:1686–1689, 2000.
- [4] R. G. Cox. The dynamics of spreading of liquids on a solid surface. Part 1. Viscous flow. *J. Fluid Mech.*, 168:169, 1986.

- [5] V. E. B. Dussan. On the spreading of liquid on solid surface: Static and dynamic contact lines. *Annu. Rev. Fluid Mech.*, 11:371–400, 1979.
- [6] L. M. Hocking. A moving fluid interface. Part 2. The removal of the force singularity by a slip flow. *J. Fluid Mech.*, 79:209–229, 1977.
- [7] C. Huh and S. G. Mason. The steady movement of a liquid meniscus in a capillary tube. *J. Fluid Mech.*, 81:401–419, 1977.
- [8] C. Huh and L.E. Scriven. Hydrodynamic model of steady movement of a solid/liquid/fluid contact line. *J. Colloid Interface Sci.*, 35:85–101, 1971.
- [9] D Jacqmin. Calculation of two-phase Navier-Stokes flows using phase-field modeling. *J. Comput. Phys.*, 155:96–127, 1999.
- [10] D Jacqmin. Contact-line dynamics of a diffusive fluid interface. *J. Fluid Mech.*, 402:57–88, 2000.
- [11] J. Koplik, J. R. Banavar, and J. F. Willemsen. Molecular dynamics of poiseuille flow and moving contact lines. *Phys. Rev. Lett.*, 60:1282, 1988.
- [12] J.J. Monaghan. Smoothed particle hydrodynamics. *Ann. Rev. Astronom. Astrophys.*, 30:543, 1992.
- [13] I. P. Natanson. *Theory of function of a real variable. Vol. II.* Frederick Ungar, New York, 2000.
- [14] T. Z. Qian, X. P. Wang, and P. Sheng. Molecular scale contact line hydrodynamics of immiscible flows. *Phys. Rev. E*, 68:016306, 2003.
- [15] Y. D. Shihkmuraev. Moving contact lines in liquid/liquid/solid systems. *J. Fluid Mech.*, 334:211–249, 1997.
- [16] P. A. Thompson and M. O. Robbins. Simulations of contact-line motion: Slip and the dynamic contact angle. *Phys. Rev. Lett.*, 63:766, 1989.
- [17] P. A. Thompson and S. M. Troian. A general boundary condition for liquid flow at solid surface. *Nature*, 389:360, 1997.
- [18] M. Y. Zhou and P. Sheng. Dynamics of immiscible-fluid displacement in a capillary tube. *Phys. Rev. Lett.*, 64:882–885, 1990.

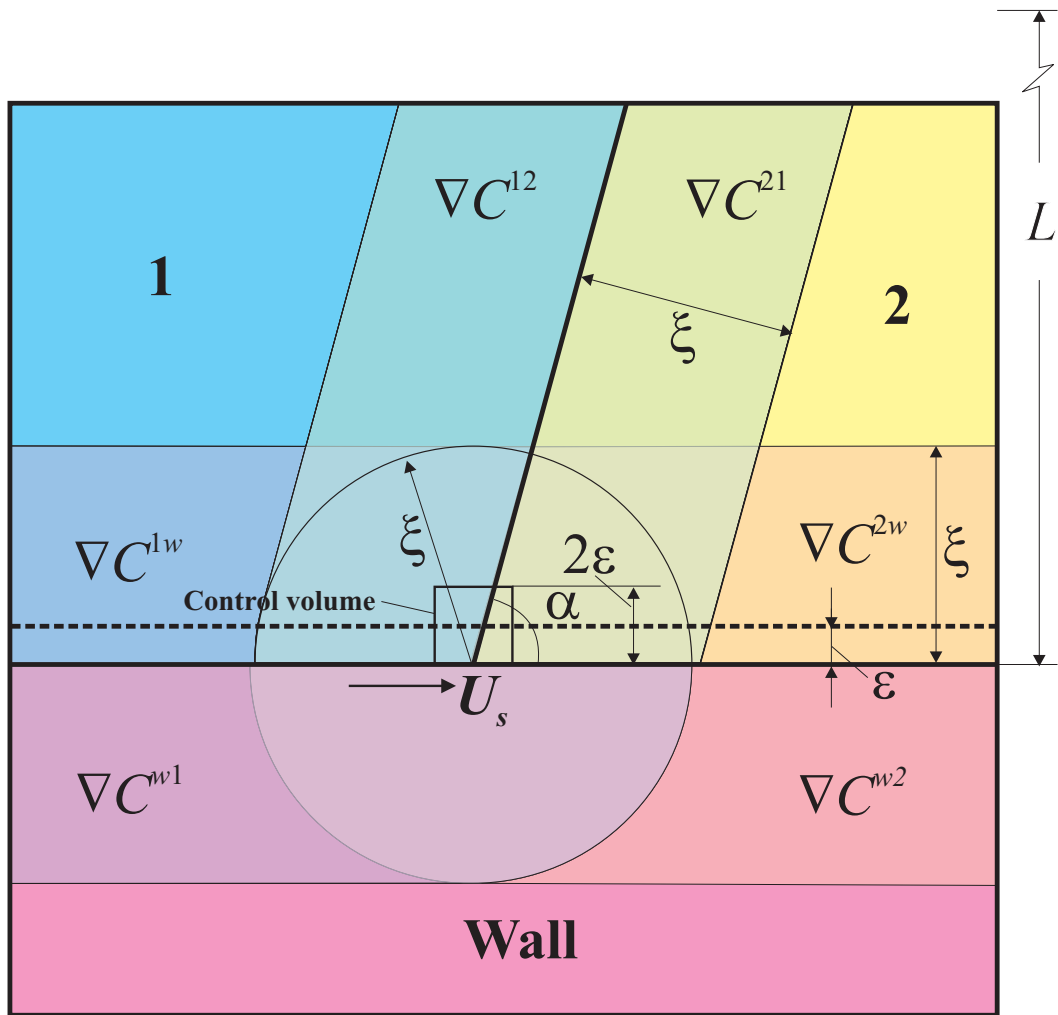


Fig. 1. smoothed, finite width interface model for moving contact line problem